

NASA Technical Memorandum 101969

# Effects of Lubrication on the Performance of High Speed Spur Gears

(NASA-TM-101969) EFFECTS OF LUBRICATION ON  
THE PERFORMANCE OF HIGH SPEED SPUR GEARS  
(NASA, Lewis Research Center) 10 pCSCL 131

N89-22919

G3/37      Unclass  
            0198666

Hachiro Mizutani and Yuuichi Isikawa  
*Mechanical Engineering Laboratory*  
*Tsukuba, Ibaraki, Japan*

and

Dennis P. Townsend  
*Lewis Research Center*  
*Cleveland, Ohio*

Prepared for the  
Fifth International Power Transmission and Gearing Conference  
sponsored by the American Society of Mechanical Engineers  
Chicago, Illinois, April 24-27, 1989

**NASA**

# EFFECTS OF LUBRICATION ON THE PERFORMANCE OF HIGH SPEED SPUR GEARS

Hachiro Mizutani and Yuuichi Isikawa  
Mechanical Engineering Laboratory  
Namiki 1-2  
Tsukuba, Ibaraki, 305 Japan

and

Dennis P. Townsend  
National Aeronautics and Space Administration  
Lewis Research Center  
Cleveland, Ohio 44135

## ABSTRACT

An experimental analysis was conducted to determine power loss and gear noise of high speed spur gears with long addendum under various conditions of load, speed, and oil jet pressure for into mesh lubrication. Power losses were calculated from temperature measurements of lubricating oil, gears, gear box, and oil flow rate. Furthermore, power loss was divided into windage loss, friction loss and churning loss. The results show that windage loss and churning loss were the main components of gear power loss of high gear speed. In addition, lubricating conditions had some influences on gear noise especially under low oil temperature or high viscosity.

## Introduction

The generation of heat, power loss and dynamics of gears are strongly related to lubricating condition. Therefore, the relationship between lubrication and power loss has been of interest and several investigators have presented data and prediction methods for gear power loss.

Ariura, Ueno, Sunaga and Sunamoto(1973) analyzed the churning loss of high speed spur gears with jet lubrication by no-load conditions. Matsumoto, Asanabe, Takano and Yamamoto(1985) derived a formula for evaluation of power loss from experimental and theoretical values. These two literatures pointed out that lubricant acceleration loss of gears was the main factor for gear power losses at high gear velocities. Anderson and Lowenthal(1979) proposed a power loss prediction method for spur-gear loss which included rolling and pumping power loss and they(1983) compared the analytical results with experimental test data. In these prediction methods, various expressions for friction, churning and windage were used, because of difficulties in simulating the lubrication mechanism or movement of oil on the tooth surfaces. Akin and Townsend(1982a,b) developed the equations for into mesh oil jet lubrications and pointed out the optimum operating condition for best lubrication and cooling from oil impingement depth.

The objective of the work described in this paper was to improve the spur-gear power loss prediction method and provide some simple assumptions for the relationship between lubrications and gear performance.

## EXPERIMENT

### TEST APPARATUS

The test apparatus is shown in Fig.1. The test gears are mounted on rigid spindles and supported by rigid pedestals. The input is direct driven by the high frequency induction motor and the output is loaded by an electric dynamometer of the eddy current type. A schematic of the gear box is shown in Fig. 2. The steel wall was 5 mm thick. The gear box was mounted on the pedestals through O-rings. Lubricant oil for the test gears was supplied by an oil pump with a heater for controlling the oil temperature. Volume of the oil tank is 200 liters. Lubricant oil was supplied to the into mesh side of the test gears by a 1mm diameter nozzle. Thermister were used to measure the 10 temperatures. Locations of the temperature measuring points were, inside of the oil inlet pipe and oil return pipe, on the side surfaces of the test gears near the tooth root, at the centers of the test gear shafts, two out of mesh locations near the edge of the gears, inside the gear box away from the walls, and outside of the gear box, as shown in Fig.2. Strain gages were located on the fillet of two teeth on the pinion. A microphone was located in the gear box for

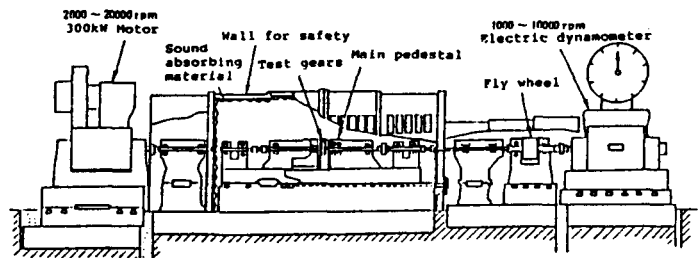


Fig.1 High speed gear tester

ORIGINAL PAGE IS  
OF POOR QUALITY

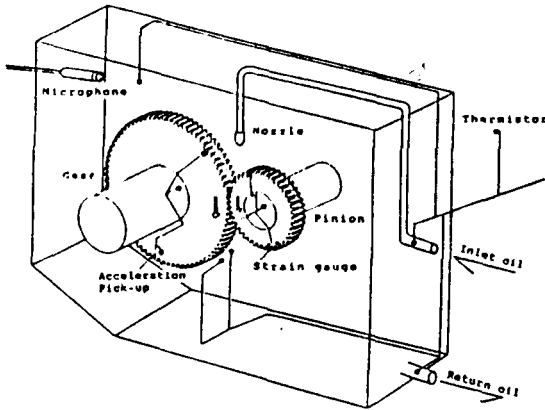


Fig.2 Schematic of the gear box

measurement of gear noise level. An accelerometer was located on the gear side surface to measure tangential acceleration.

TEST GEARS

Dimensional specifications of the test gears are listed in Table 1. Tooth profiles of the test gears and single flank rolling errors are shown in Fig. 3. The middle part of the tooth profile was ground. The parts near tip and root were unground and had a large tip and root relief for eliminating edge contacts at the start and end of tooth engagement. The effects of these large reliefs were apparent on single flank rolling error, shown in Fig. 3. Addendum ratio of the gears is 1.2 and total tooth height is 2.7 module. The contact ratio calculated theoretically without relief was 2.2. However, actual contact ratio of the gears is about 1.3 because of the large relief. Clearance space at the tooth root is considerably small. Therefore, the ratio of maximum to minimum space between meshing teeth is 30% larger than that of a standard gear pair with normal tooth height.

Table 1 Test gears

Module	m	3
Pressure angle	$\alpha$	20°
Number of tooth	z	40
	z	77
Face width	b	25mm
Addendum modificatio		no
Tooth hight	h	2.7 module
Tip & root relief		200 $\mu$ m
Height of tip relief		1.1mm
Contact ratio	$\epsilon$	2.0
Processing		Grinding
Roughness of tooth Surface		1.5~2 $\mu$ m
Accuracy		JIS Class 0

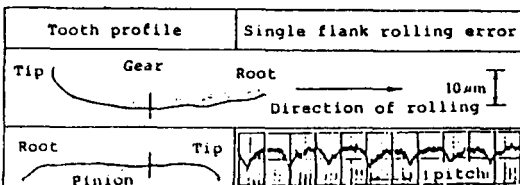


Fig.3 Tooth profile and single flank rolling error

EXPERIMENTAL PROCEDURES

Operating conditions are shown in Table 2. Rotational speed was increased in steps of 1000 rpm. The oil flow rate of the jets was calibrated at an oil inlet temperature range of 16-50 °C by linearly increasing the oil pressure. Then, the oil pressure was selected as the index of oil flow rate. Maximum AGMA K-factor in this experiment was equal to 1180 at the driven shaft torque of 392Nm. The operation was started with low rotational speed, low load and high oil flow rate. After a rotational speed and a torque were fixed, the oil pressure was changed from 0.59MPa to 0.20MPa in the steps of 0.10MPa. Temperature, strain, noise, and vibration were measured at 10 second interval. The fluctuation in inlet oil temperature was less than  $\pm 0.03$  °C during operation at a set rotational speed and torque. Averages of the 3 measured values were recorded at 30 second intervals. When the rate of change of temperature on the side surface of the pinion tooth was less than 0.06 °C/min, at every operating condition, the final data were recorded.

Temperatures were measured at 6rpm with no load and with 0.59MPa oil pressure for analyzing the thermal conduction to the gears and through the gear box.

RESULTS

DYNAMIC CHARACTERISTICS OF THE GEARING SYSTEM

The calculated resonant frequency of the test gears is 3200Hz and the critical speed is 4800rpm. Fillet strains were influenced by the resonance of the gearing system around 5000rpm as shown in Fig.4. Variation of strain was small above 8000rpm. The strain at 6000rpm was 14% higher than the strain at 10,000rpm. Strains at the end of tooth contact at 3000rpm and 4000rpm were 10% higher and strain at the start of tooth contact at 5000rpm was 23% higher than those at 10000rpm.

TEMPERATURE AND ROTATIONAL SPEED

Fig.5 shows a transient rise in temperatures at a rotational speed of 12000rpm, torque 196Nm, inlet oil temperature 29.0°C, after the inlet oil pressure was reduced from 0.29MPa to 0.20MPa. The inlet oil, shaft

Table 2 Operating condition

Backlash	300 $\mu$ m
Rotational speed	3000~12000rpm
Pitch line speed	18.8~75.4m/s
Tooth load	452N, 1807N, 3615N
Torque of driven shaft	49Nm, 196Nm, 392Nm
Lubricant	ISO VG32 (EP Turbine oil #90)
Temperature of inlet oil	28°C and 22°C for 9000rpm
Viscosity of oil at 28°C	52cSt
Diameter of nozzle	1mm
Inlet oil pressure	0.20, 0.29, 0.39, 0.49, 0.59 MPa
Oil flow rate at 28°C	1.3, 1.7, 2.1, 2.5, 2.9 l/min
Velocity of oil jet	27, 35, 45, 53, 62 m/sec
Direction of oil jet	Into mesh

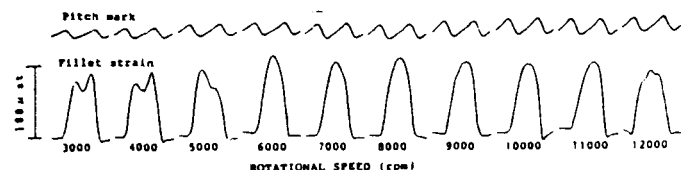


Fig.4 Fillet strain under the driven shaft torque 392Nm

temperature and ambient air were nearly constant. All other temperatures rose with time, and each one came up to a stabilized point. The temperature rise of the gears and oil after about 5 minutes was nearly equal to each other. The temperature of the pinion tooth was the highest of all on every running condition. The temperature differences between the pinion and gear teeth and shafts were fairly large, as a result of the sizes of the gears and the conditions of the support bearings.

Fig.6 shows the temperature rise of the gears and oil from the initial oil inlet temperature versus rotational speed at the driven shaft torque of 392Nm, inlet oil pressure 0.39MPa, and inlet oil temperature  $28 \pm 1$  °C. Temperatures of the pinion teeth at lower speeds from 3000rpm to 6000rpm were somewhat high as a result of gear dynamics shown in Fig. 4. The temperature of the oil mist in the gear box and return oil increased in parallel to the temperature of the gears with increasing speed. The temperature of the oil jet increased along with the temperature of the gear tooth at all speeds.

The effect of oil pressure on the pinion tooth temperature with increasing speed is shown in Fig. 7. At 3000rpm and 4000rpm, oil pressure had little effect on pinion tooth temperature. At higher speeds reduced oil pressure caused an increase in temperature. However, at oil pressure over 0.39 MPa, a smaller cooling effect of the pinion tooth was found. The temperature of the return oil rose with speed similar to pinion temperature as shown in Fig. 8. However, the influence of the resonance of the gearing system on temperature could not be seen in Fig. 8.

THERMAL CONDUCTION OF GEARS AND CONVECTION OF GEAR BOX

Power loss, initiated by gear tooth meshing, is converted to heat. The heat is taken away by the lubricant oil and the gears. Part of the heat in a gear box is transferred by convection through the gear box. When calculating gear power loss by means of temperature measurement, it is necessary to include the thermal conductions of the gears and the convection of the gear box. In this study, the temperature distribution of the gear box measured with test conditions of 6rpm, no load, 0.59MPa oil pressure, and several inlet oil temperatures. One of the temperature distribution is shown in Fig. 9. The differences in the temperatures between inlet oil and return oil shows the quantity of heat flowing through the gears and gear box. Heat flow through the gears was expressed as follows:

$$Q = 2\lambda(T_p - T_s)B / \ln(D_p - D_s)$$

- Where, Q : Quantity of heat (W)
- D<sub>p</sub>: Diameter of pitch circle (m)
- D<sub>s</sub>: Diameter of gear shaft (m)
- T<sub>p</sub>: Temperature of gear tooth (°K)
- T<sub>s</sub>: Temperature of gear shaft (°K)
- λ: Thermal conductivity (W/m/°K)
- B : Tooth width (m)

In this expression, thermal conduction of the gear side surfaces are neglected. By subtracting the quantity of heat for the gears from the total quantity of heat, the quantity of heat for the gear box only was found and was transferred to the overall heat transfer coefficient of the gear box. This coefficient has the dimension of [kcal/m<sup>2</sup>/h/°C], and is shown in Fig.10 versus the difference in temperature between the mist in the gear box and the room air. The mean value of the data is 7.5. This value was used for the following calculations of the power losses of the test gears.

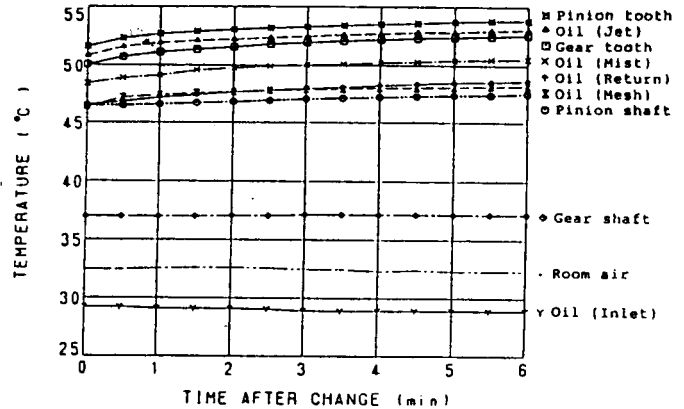


Fig.5 Rising transition of temperature about the gears and oil at 12000rpm and 196Nm after changing oil pressure from 0.29MPa to 0.20MPa

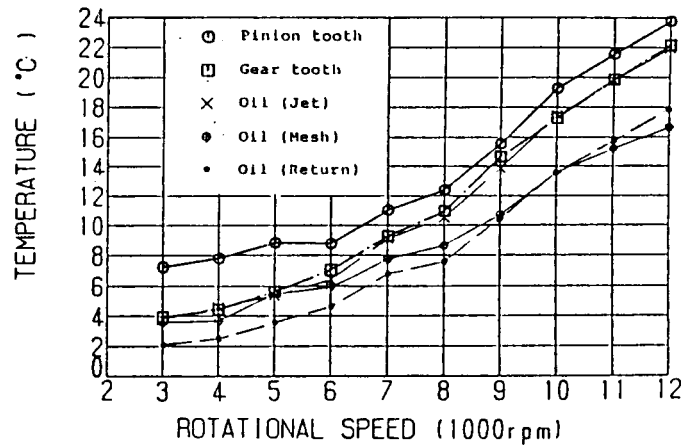


Fig.6 Rising temperatures of the gear teeth and oils from inlet oil temperature at oil pressure 0.39MPa and torque 196Nm

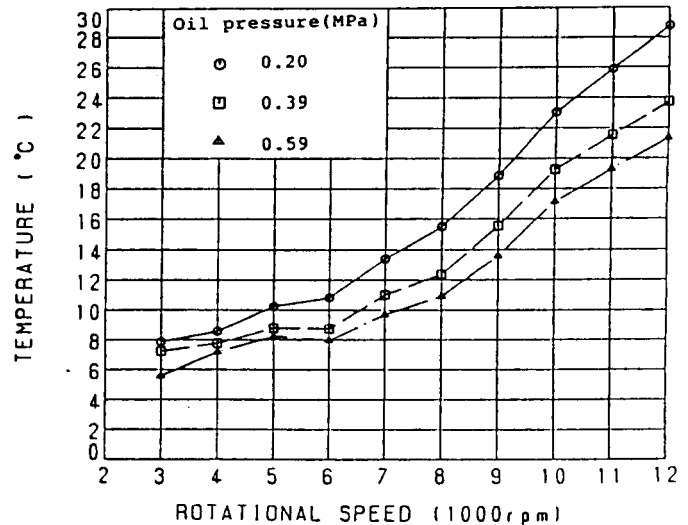


Fig.7 Rising temperature of the pinion tooth under 196Nm

**POWER LOSS OF THE GEARS**

The experimental results of gear power loss are shown in Fig.11 and Fig.12. Power loss increases with speed, load and oil pressure as shown in Fig.11. The percent power loss with a torque of 392Nm was nearly constant with increasing speed and oil pressure and close to the percent loss at the 196Nm torque. Power loss with the light 49Nm torque was sensitive to speed

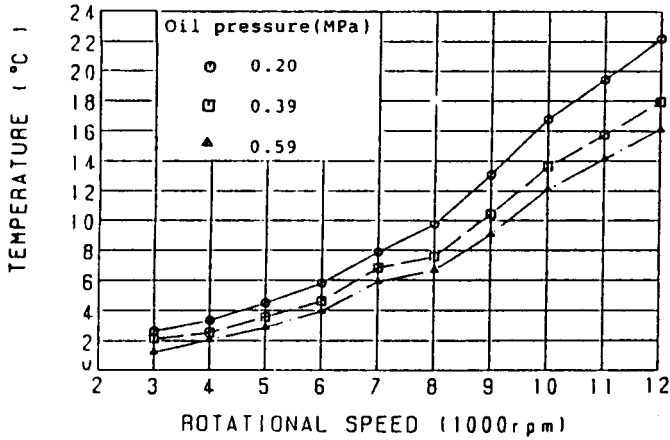


Fig.8 Rising temperature of return oil under

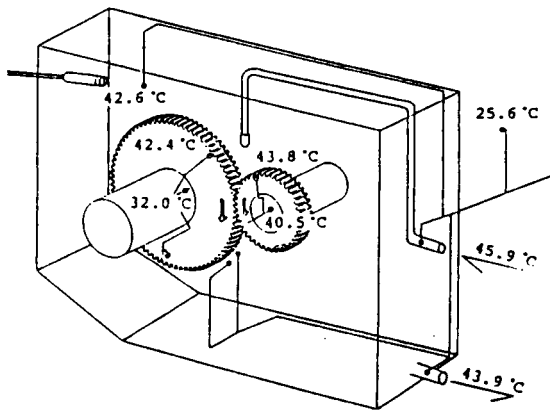


Fig.9 Thermal distribution in the gear box at 6rpm and oil pressure 0.59MPa and no load

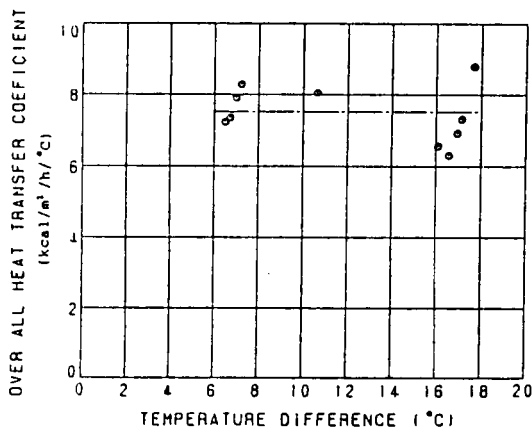


Fig.10 Over all heat transfer coefficient of the gear box between ambient and oil mist inside gear box

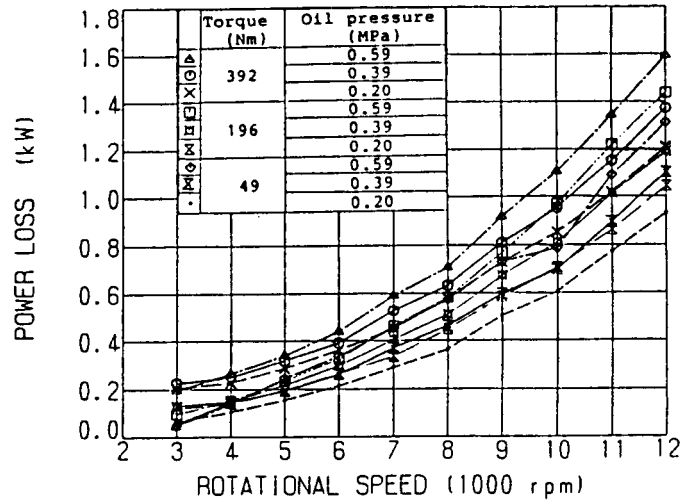


Fig. 11 Power loss of the gears

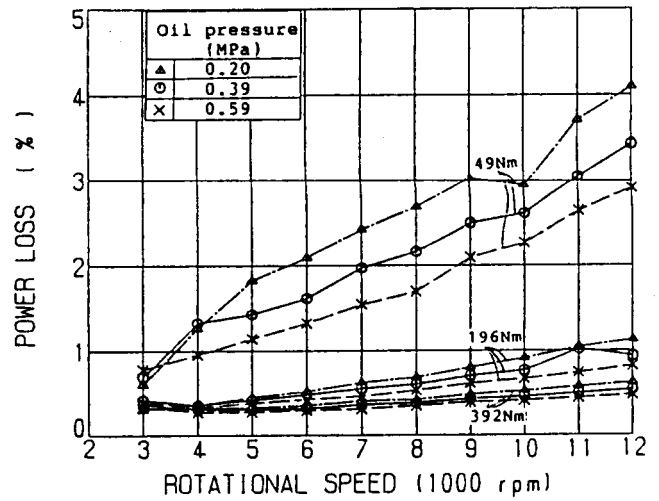


Fig.12 Percent power loss of the gears

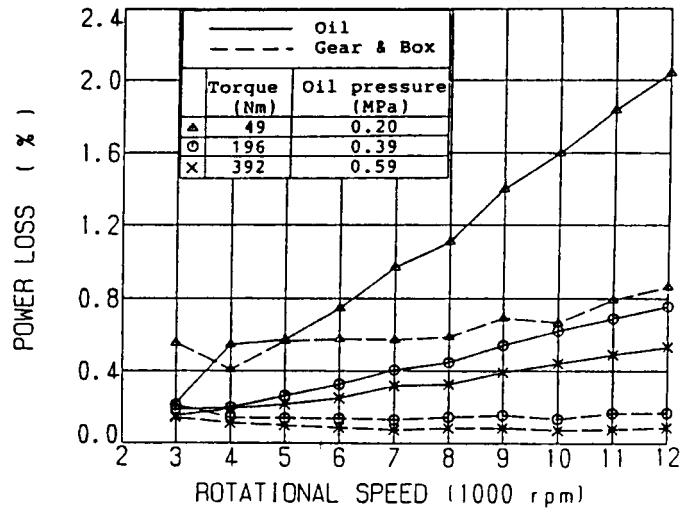


Fig.13 Percent power loss based on temperature differences of inlet oil and return oil, and on heat transfer of the gears and the gear box

as shown in Fig.12. Fig.13 shows the percent power loss divided into two areas. One is the percent calculated by temperature difference between the return oil and inlet oil. The other is the percent calculated by heat transfer through the gears and the gear box. These latter percent power losses were nearly constant with speed. This shows that the estimation of the partial power loss calculated by heat transfer through the gears and the gear box has little influence on the total power loss of gears at high speeds and high loads. Plots of power loss versus torque at several speeds and oil jet pressures are shown in Fig.14. Plots of power loss versus oil pressure at several speeds and torques are shown in Fig.15. Power loss was proportional to torque and oil pressure at all speeds.

**ANALYSIS AND DISCUSSION**

In this analysis of power loss, it was assumed that the sources of power loss for gears are windage, friction, and churning. Friction loss could be broken into sliding loss and rolling loss. These losses were combined in the measured data. The total power loss PL is expressed in the following formula as a function of speed, load and oil pressure.

$$PL = PL_w + PL_f + PL_c = F(n, l, p)$$

- where, PL<sub>w</sub>: Windage loss
- PL<sub>f</sub>: Friction loss
- PL<sub>c</sub>: Churning loss
- n: Rotational speed
- l: Driven shaft torque
- p: Oil pressure

Since the power losses at all speeds have a linear relationship with load and oil pressure respectively, as shown in Fig. 14 and Fig. 15, windage loss can be defined as loss under no load and no oil supply. This loss and other losses are expressed as the following formula.

For windage loss:  $PL_w = F(n, 0, 0)$

For friction loss:  $PL_f = F(n, l, p) - F(n, 0, p)$

For churning loss:  $PL_c = F(n, l, p) - F(n, l, 0)$

where, function F(n,0,p) is power loss under no load and function F(n,l,0) is the power loss under no oil supply. The power loss F(n,0,l) and F(n,l,0) were deduced by least square method.

**WINDAGE LOSS**

The windage loss when separated from the power loss, increased exponentially with rotational speed as shown in Fig.16. This loss is in good agreement with a curve of  $n^{2.3}$ . The exponent 2.3 is smaller by 0.5 than the value presented by Anderson and Lowenthal (1979).

**FRICITION LOSS**

The friction loss with torques of 196Nm and 392Nm decreased slightly from 3000 to 5000rpm and increased with speeds over 6000rpm as shown in Fig.17. This decrease appears to be the effects of increased elastohydrodynamic oil film thickness. The friction loss under the light torque remained low even at high speeds. These friction losses decreased slightly with oil pressure except at 10000rpm. The mean coefficient of friction, calculated backward from the

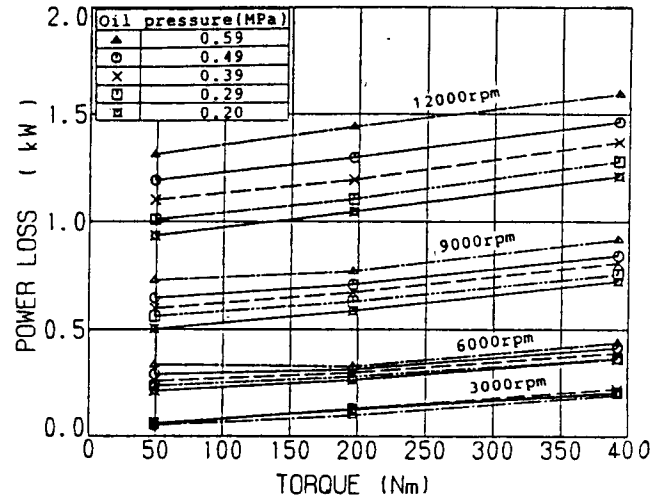


Fig.14 Power loss versus torque four speeds and five oil inlet pressures

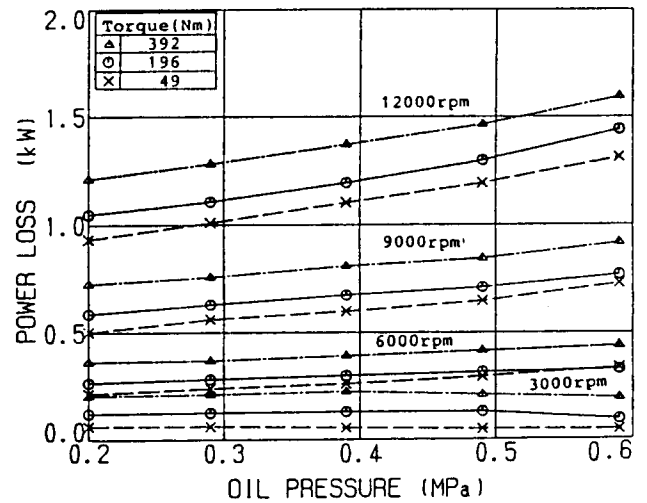


Fig.15 Power loss versus inlet oil pressure for four speeds and three torques

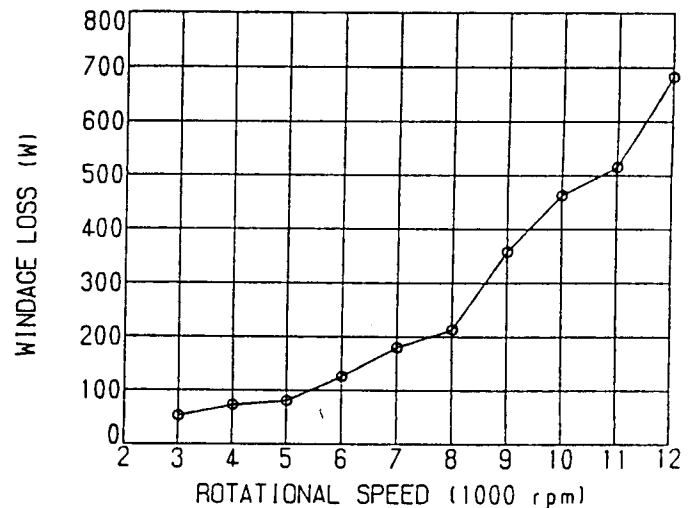


Fig.16 Windage loss versus gear speed

power loss by using the formula of Shipley (1962), were about 0.02 at 3000rpm and 0.01 over 5000rpm as shown in Fig.18. These coefficients are smaller than values currently used and those shown by Shipley (1962).

**CHURNING LOSS**

The churning loss increased in proportion to speed and oil pressure as shown in Fig.19. The main sources of churning power loss are, oil acceleration by the gear teeth and pumping loss in the mesh as the oil is trapped between the meshing teeth. If the loss by oil acceleration is the main source of churning loss, then an oil jet tangential velocity equal to the gear pitch line velocity would reduce the loss to near zero. The

velocities of the oil jet at 0.39MPa and 0.59MPa were equal to the pitch line velocities at 7000rpm and 10000rpm, respectively. Since the losses shown in Fig.19 were not significantly reduced where the jet velocity was equal to pitch line velocity, it is concluded that the main source of churning loss was the pumping or mixing of the oil in the meshing teeth. A rough percentage ratio of jet oil to mesh oil was calculated by using the temperatures of the jet oil, mesh oil and return oil in the following formula.

$$\text{Ratio of jet oil} = (Tr+Trb-Tm)/(Ts-Tr-Trb)*100 (\%)$$

Where, Tr :temperature of return oil

Tm :temperature of mesh oil

Ts :temperature of jet oil

Trb:equivalent temperature change of

return oil to heat flow of gear box

The curves of the percentage ratio of jet oil shown in Fig.20 have a minimum around 0.39MPa at higher speeds of 11,000 and 12,000rpm. This indicates that oil passes through the mesh with the least loss at an oil jet pressure of 0.39MPa as compared to the loss at higher and lower pressures. Therefore, the results from Fig.7 and Fig.20 shows that the oil jet pressure of 0.39MPa is the best condition for minimum power loss.

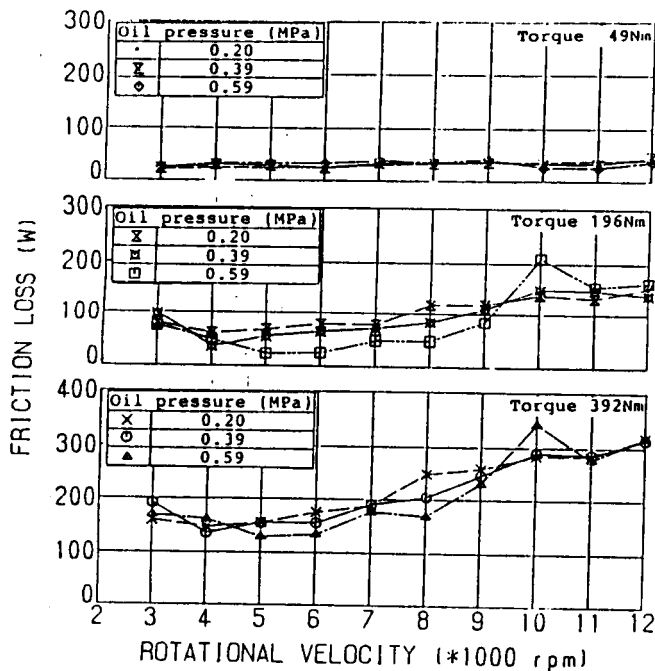


Fig.17 Friction loss versus gear speed at three torques and oil inlet pressures

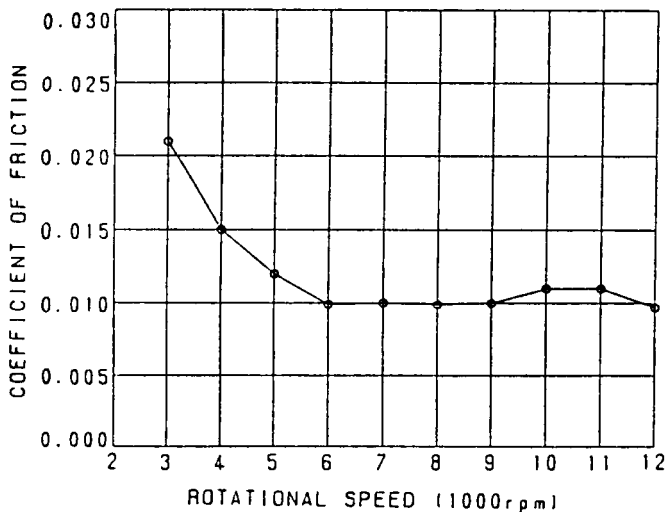


Fig.18 Coefficient of friction versus gear speeds

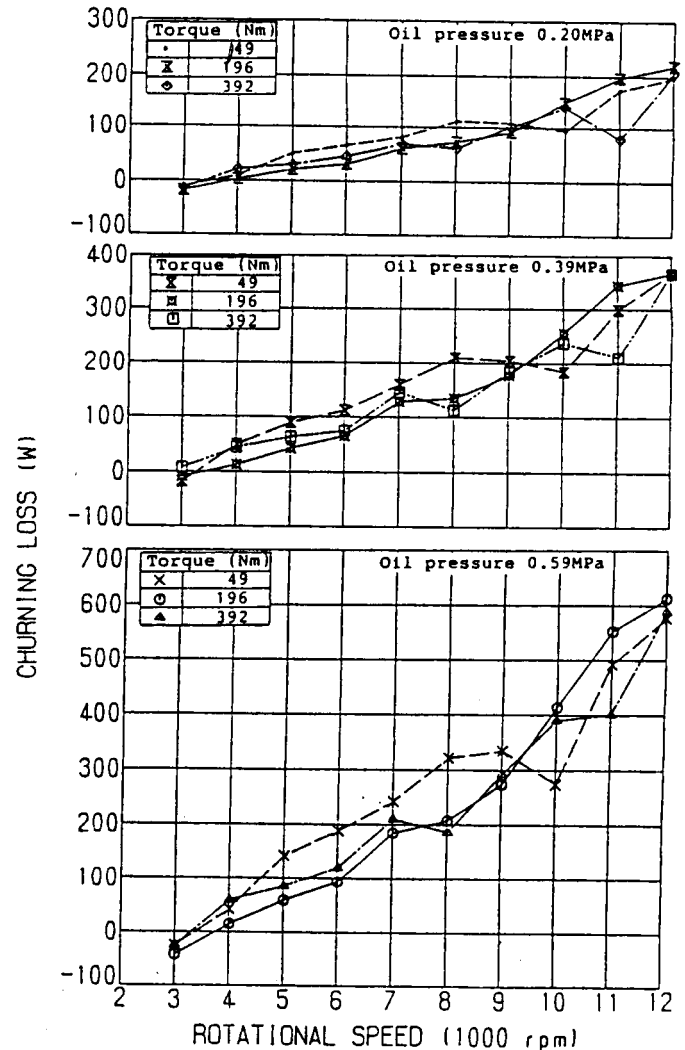


Fig.19 Churning loss versus gear speed at three torques and inlet oil pressures

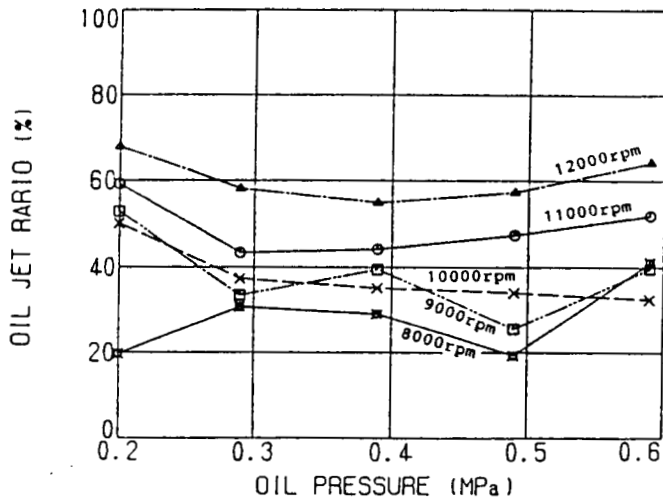


Fig.20 Ratio of jet oil to mesh oil

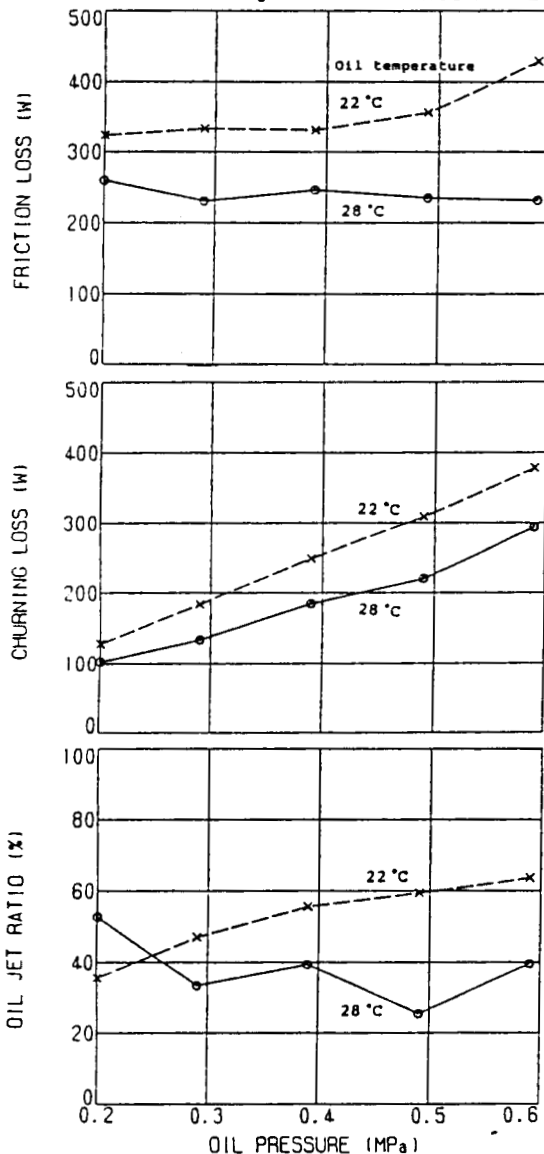


Fig.21 Influences of inlet oil temperature on friction loss, churning loss and ratio of jet oil at 9000 rpm and 392Nm

### INFLUENCE OF INLET OIL TEMPERATURE

The influences of inlet oil temperatures on the friction loss, churning loss and the oil jet ratio are shown in Fig.21. The viscosity of the oil at 22 °C and 28 °C were 70 cSt and 53 cSt respectively. The lower oil temperature caused an increase in power loss and oil jet ratio at nearly all oil jet pressures. A significant change in gear noise level also occurred with oil pressure as shown in Fig.22. Fig.23 shows the spectrum of the gear noise at an inlet oil temperature of 22 °C and 9000 rpm with 392Nm torque and three oil jet pressures. High noise level at an oil jet pressure of 0.2MPa could be due to insufficient oil on the tooth surfaces. Increased noise levels at the second and the third harmonics of the meshing frequency with higher oil pressure, shown in Fig.23, were related to oil jet ratio. The level of noise around the meshing frequency ( $f_z$ ) was lower at an oil temperature of 28 °C than it was at 22 °C. No influences of oil temperature and oil pressure on gear vibration was observed in this experiment.

### SUMMARY

High speed tests were conducted with long addendum spur gears under various test conditions of gear speed, tooth load, and oil pressure for into mesh lubrication. Power loss of the gears was calculated from temperature differences between inlet oil and return oil, between gear tooth and gear shaft, and between mist in the gear box and ambient air outside of the gear box. Windage, friction, and churning power loss were analyzed by extrapolating power loss with no-load and/or no oil supply. A rough estimation of oil movement in the meshing teeth was determined from oil temperatures. Power loss and gear noise were compared at two test conditions with different inlet oil temperature. The following results were obtained.

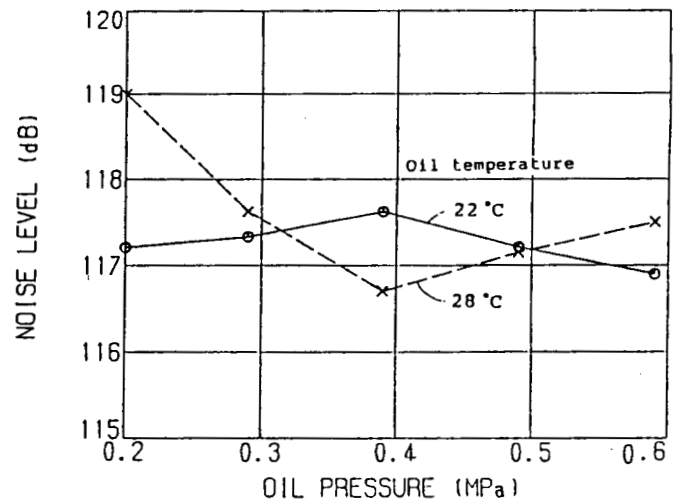


Fig.22 Gear noise level and inlet oil pressure at 9000 rpm and 392Nm for two inlet oil temperature

(1) Gear power loss was proportional to tooth load and rate of oil flow at all gear speeds.

(2) The main sources of gear power loss at high gear speeds were found to be windage and churning.

(3) Pumping or mixing of oil and mist in the meshing teeth was the main source of churning loss.

(4) The ratio of jet oil to oil carried through the mesh can be influenced by the rate of oil flow and viscosity.

(5) Gear noise level at the first, second, and third harmonics of the meshing frequency were influenced by lubricant temperature and viscosity.

(6) An additional temperature rise of the gear tooth was observed around the resonant speed of the gear system. However, increased power loss at resonant speed was negligible.

#### REFERENCES

Akin, L. S. and Townsend, D. P., 1982, "Into Mesh Lubrication of Spur Gears With Arbitrary Offset Oil Jet I-For Jet Velocity Less Than or Equal to Gear Velocity," NASA TM-83040

Akin, L. S. and Townsend, D., P., 1982, "Into Mesh Lubrication of Spur Gears with Arbitrary Offset Oil Jet II-For Jet Velocity Equal to or Greater Than Gear Velocity," NASA TM-83041

Anderson, N. E., and Lowenthal, S. H., 1979, "Par and Full Load Spur Gear Efficiency," NASA TP-1622, AVRADCOM TR79-46

Anderson, N. E., and Lowenthal, S. H., 1983, "Comparison of Spur Gear Efficiency Prediction Methods," NASA Conf. Publ. No. NASA-CP-2210

Ariura, Y., Ueno, T., Sunaga, T. and Sunamoto, S., 1973, "The Lubricant Churning Loss in Spur Gear System," Bulletin of JSME Vol.16 No.95, May

Matumoto, S., Asanabe, S., Takano, K. and Yamamoto, M., 1985, "Evaluation Method of Power Loss in High-Speed Gears," Proceedings of JSLE International Tribology Conference

Sipley, E. E., 1962, "Loaded Gears in Action," Gear Handbook, D. W. Dudley ., McGraw Hill Book Co., Inc.,

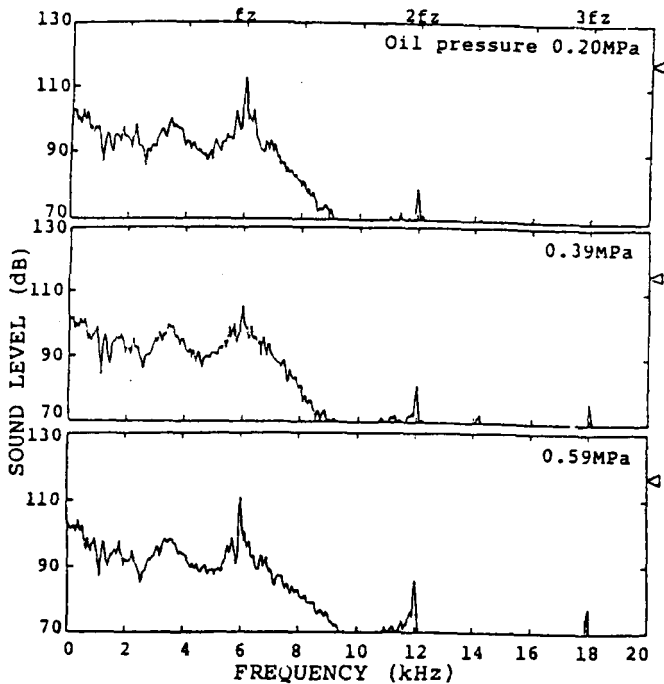


Fig.23 Spectrum of the gear noise at 9000rpm, 392Nm and inlet oil temperature 22 C



# Report Documentation Page

1. Report No. NASA TM-101969		2. Government Accession No.		3. Recipient's Catalog No.	
4. Title and Subtitle Effects of Lubrication on the Performance of High Speed Spur Gears				5. Report Date	
				6. Performing Organization Code	
7. Author(s) Hachiro Mizutani, Yuuichi Isikawa, and Dennis P. Townsend				8. Performing Organization Report No. E-4666	
				10. Work Unit No. 505-63-51	
9. Performing Organization Name and Address National Aeronautics and Space Administration Lewis Research Center Cleveland, Ohio 44135-3191				11. Contract or Grant No.	
				13. Type of Report and Period Covered Technical Memorandum	
12. Sponsoring Agency Name and Address National Aeronautics and Space Administration Washington, D.C. 20546-0001				14. Sponsoring Agency Code	
15. Supplementary Notes Prepared for the Fifth International Power Transmission and Gearing Conference sponsored by the American Society of Mechanical Engineers, Chicago, Illinois, April 24-27, 1989. Hachiro Mizutani and Yuuichi Isikawa, Mechanical Engineering Laboratory, Namiki 1-2, Tsukuba, Ibaraki, 305 Japan; Dennis P. Townsend, NASA Lewis Research Center.					
16. Abstract An experimental analysis was conducted to determine power loss and gear noise of high speed spur gears with long addendum under various conditions of load, speed, and oil jet pressure for into mesh lubrication. Power losses were calculated from temperature measurements of lubricating oil, gears, gear box, and oil flow rate. Furthermore, power loss was divided into windage loss, friction loss and churning loss. The results show that windage loss and churning loss were the main components of gear power loss of high gear speed. In addition, lubricating conditions had some influences on gear noise especially under low oil temperature or high viscosity.					
17. Key Words (Suggested by Author(s)) Lubrication gears; High speed; Efficiency; Friction loss; Windage loss; Churning loss; Vibration; Gear noise			18. Distribution Statement Unclassified - Unlimited Subject Category 37		
19. Security Classif. (of this report) Unclassified		20. Security Classif. (of this page) Unclassified		21. No of pages 10	22. Price* A02